Copyright Warning & Restrictions

The copyright law of the United States (Title 17, United States Code) governs the making of photocopies or other reproductions of copyrighted material.

Under certain conditions specified in the law, libraries and archives are authorized to furnish a photocopy or other reproduction. One of these specified conditions is that the photocopy or reproduction is not to be "used for any purpose other than private study, scholarship, or research." If a, user makes a request for, or later uses, a photocopy or reproduction for purposes in excess of "fair use" that user may be liable for copyright infringement,

This institution reserves the right to refuse to accept a copying order if, in its judgment, fulfillment of the order would involve violation of copyright law.

Please Note: The author retains the copyright while the New Jersey Institute of Technology reserves the right to distribute this thesis or dissertation

Printing note: If you do not wish to print this page, then select "Pages from: first page # to: last page #" on the print dialog screen

ABSTRACT

Characterization of three-dimensional shear flows

by

Kurra Bhaswan

This work investigates techniques to analyze and characterize the presence of microstructure in moderately dilute three-dimensional shear flows. In three dimensional shear flows, a distinct structure develops as the coefficient of restitution is lowered with the particles exhibiting a strong tendency towards the formation of clusters. There exists a need to automatically detect and characterize this microstructure in the given flow. Several methods are examined for effective characterization of the microstructure. The techniques employed are based on the classification of the data based on the properties of the Voronoi diagram constructed from the positional parameters of the two-dimensional slices of the 3d shear flows and on the extraction of quantitative descriptors from determining the fractal dimension.

The fractal nature of the microstructure in three-dimensional shear flows lends itself to the application of several measures of the fractal dimension. The self-similarity property of fractals makes the fractal dimension particularly effective in distinguishing between nuances in the structure. The geometrical properties of Voronoi and Delaunay tessellations help describe the neighborhood of particles. In such a scheme, the statistics gathered from the properties involving the proximity relationships between particles is particularly significant because of the proven tendency of the particles to form clusters. The scheme involves discriminating between the statistical parameters obtained from the measures of the Voronoi polygons and Delaunay triangles.

Methods such as the Fourier Transform techniques and variance analysis, shown by other researchers have suffered from either being severely computationally intensive or being relatively weak in discriminating between nuances in the miscrostructure. The techniques discussed are shown to be computationally efficient and to be successful in characterizing the microstructure. Thus a potentially effective set of methods are introduced that may be adapted to better detect and characterize the microstructure and may also be extendible to other spatial data analysis situations.

CHARACTERIZATION OF THREE-DIMENSIONAL SHEAR FLOWS

by

Kurra Bhaswan

A Thesis
Submitted to the Faculty of
New Jersey Institute of Technology
in Partial Fulfillment of the Requirements for the Degree of
Master of Science in Computer Science

Department of Computer and Information Science

October 1993

APPROVAL PAGE

Characterization of Three-Dimensional Shear Flows

by

Kurra Bhaswan

Dr. Rajesh N. Dave, Thesis Advisor — Date
Associate Professor of Mechanical Engineering, NJIT

Dr. James A. M. McHugh, Committee Member — Date
Full Professor of Computer and Information Science, NJIT

Dr. Dao C. Hung, Committee Member — Date
Assistant Professor of Computer and Information Science, NJIT

BIOGRAPHICAL SKETCH

Author: Kurra Bhaswan

Degree: Master of Science in Computer and Information Science.

Date: October 1993

Undergraduate and Graduate Education:

- Master of Science in Computer and Information Science,
  New Jersey Institute of Technology, Newark, NJ, 1993
- Master of Science in Mechanical Engineering,
  New Jersey Institute of Technology, Newark, NJ, 1991
- Bachelor of Science in Mechanical Engineering,
  J.N.T.U College of Engineering, India, 1988

Major: Computer and Information Science.

Publications:

Dave, R. N., and Bhaswan, K., "Adaptive Fuzzy c-shells Clustering and Detection of Ellipses", *IEEE Trans. on Neural Networks* 3(5) (1992)

Dave, R. N., and Bhaswan, K., "New Measures for evaluating fuzzy partitions induced through c-shells clustering", *Intelligent Robots and Computer Vision IX*: Algorithms and Techniques, an SPIE conference, 12-17 November 1991, Boston, MA.

Dave, R. N., and Bhaswan, K., "Adaptive c-shells clustering", *Proceedings of the North American Fuzzy Information Processing Society Workshop*, Columbia, Missouri, *pp.* 195-199, 1991

This thesis is dedicated

to my parents

ACKNOWLEDGMENT

I take this opportunity to express my deep gratitude to Dr. Rajesh N. Dave, Associate Professor, Mechanical Engineering Department of NJIT. for his encouragement and valuable guidance throughout the course of this work. His helpful hints, suggestions and patience were of immense help.

I am also very thankful to Dr. James McHugh and Dr. Dao Hung for their valuable guidance and for providing me with useful suggestions.

TABLE OF CONTENTS

Chapter Page

LIST OF FIGURES

Figure **Page**

LIST OF TABLES

Table Page

CHAPTER 1
INTRODUCTION

1.1 Objective

In recent years a substantial increase of interest in the granular flow of materials has been seen. It can be applied to many industrial fields, such as in-plant and long-distance transport, manufacturing ceramics, casting of solid-fuel rocket propellant, pharmaceuticals, plastics, materials development, food, mineral processing operations and natural geological flows [1]. Lack of understanding the material property of the granular flows makes scaling from laboratory bench-top prototype operations to large-scale commercial plants very difficult. It is more of a "cut-and-try" art than a reasonable design process [2]. The highly nonlinear nature of the granular flow poses enormous difficulties in developing constitutive models to predict behavior over a range of conditions. Campbell [3] observed the formation of a distinct layered structure in particle simulations of very dense shear flows. Hopkins and Louge [4] described a dynamic micro-structure in simulations of two-dimensional shear flows of uniform disks caused by inelastic collisions. This inelastic micro-structure was characterized by dynamic clusters of disk on the order of 10 diameters in size. However the prevalent methods are weak and there exists a need for a better method to characterize the microstructure in three dimensional shear flows. The objective of this work is to investigate methods and techniques to characterize the microstructure present in moderately dilute three-dimensional shear flows. The emphasis is primarily on characterizing the miscrostructure. In doing so, the approach has been one of examining available methods currently being used and the investigation of techniques particularly suited to the problem on hand. The main requirements in such a process involve employing methods that are computationally efficient, fairly robust, discriminatory and are naturally applicable to the task of detection of microstructure.

1.2 Methods/Techniques

In the past, the methods to characterize the microstructure in the three-dimensional shear flows employed Fourier Transform techniques and Variance analysis techniques. These methods were based on certain assumptions. The Fourier transform technique is an accepted and effective method, but is computationally intensive and therefore not suitable for practical analysis of data. The variance analysis technique is prone to errors resulting from improper grid size and is unstable on account of its simplicity. It is particularly suspect when the grid size is arbitrarily chosen. The approach in this work has been to at least avoid the problems encountered by the methods mentioned above and to be able to provide new and efficient means of characterizing the resulting microstructure.

1.3 Criteria for the methods employed

The criteria that were used in choosing the methods may be listed as follows:

a) computationally efficiency.

b) robustness.

c) consistency and accuracy.

d) extensibility of the method/technique to other data analysis situations.

1.4 Overview of the Remaining Chapters

The next chapter examines some of the methods developed by researchers in the past and other methods that seem applicable.

Chapter 3 introduces the concept of the fractal dimension and discusses several measures of the dimension and the results from their application.

Chapter 4 discusses the construction of the Voronoi Diagram, its properties and the classification of the data based on the utilization of the second order statistics of the geometry resulting from the tessellation along with a discussion of the results.

Chapter 5 concludes the work and points to directions for future research.

Appendix A gives a brief overview of object oriented design employed in the implementation of the voronoi diagram.

Appendix B contains a brief description of the fundamental data structure used to store the information contained in the Voronoi diagram *viz.* the doubly connected edge list.

Appendix C contains plots for the variance analysis scheme employing different grid dimensions.

Appendix D contains histogram plots for two cases resulting from the geometrical properties of the Voronoi diagram.

CHAPTER 2

BACKGROUND

2.1 Introduction

This section examines the techniques used in the past and examines other techniques applicable to the problem on hand. The methods for classification were chosen based on the fact that the microstructure associated with the data resulting from three dimensional shear flows had some periodicity associated with it and is therefore suited to being exploited by methods that can extract characteristics from spatial analysis of the data. We start by describing the conditions under which the microstructure develops and observations made by other researchers regarding the nature of such flows. We briefly examine two of the methods used in the past and finally examine alternatives in the form of geometric methods that can be used.

2.2 The nature of granular shear flows

Cambell[3] observed the formation of a distinct microstructure created by the layering of densely packed disks undergoing shear. In molecular dynamics, computer simulations have also revealed microstructures characterized by anisotropic radial distribution functions, which are perturbations to the equilibrium isotropic radial distribution function caused by the imposed mean shear field. The fundamental microstructure, which is present to some degree in all granular flows of disks, depends on the dissipation of energy by inelastic collisions which will be referred to as inelastic microstructure.

The basic feature of inelastic microstructure is the formation of local, anisotropic regions of particle concentration above and below the bulk average. As a result of these fluctuations in concentration, the stresses and other statistical measures of the flow may differ significantly from the values predicted by theories that postulate spatial homogeneity. Further, the results of computer simulations of simple shear flows will depend on the size of the periodic domain relative to the size of the microstructure: small domains may

inhibit the formation of inelastic microstructure.

Particle simulations have been extensively used in numerical experiments with granular flows. Parametric studies of rapidly sheared granular flows have been performed by several researchers. Implicit in these studies is the assumption that given a reasonable number of particles, the statistical measures of the flow are independent of the size of the periodic domain. In this work we use the data obtained from computer simulation of particles. We used the code provided by Kim[5] to obtain data to be processed by the classification schemes proposed herein.

2.3 Fast Fourier Transform

The Fourier Transform[7] is one of the most popular measures because the idea of decomposing a non-periodic signal into a a set of sinusoidal or harmonic signals is widely known among scientists and engineers. The assumption made in this method is that the periodic or non-periodic signal can be represented as a synthesis of sine or cosine signals

$$f(t) = \frac{1}{2\pi}\int_{T} F(\omega)\, e^{i\omega t} d\omega$$

where $e = \cos\omega t + \sin\omega t$

Since $F(\omega)$ is often complex, the absolute value of $|F(\omega)|$ is used in graphical displays. When the motion is periodic or quasiperiodic, $|F(\omega)|$ shows a set of narrow spikes or lines indicating that the signal can be represented by a discrete set of harmonic functions $\{e^{\pm i\omega_k t}\}$, where $k = 1, 2, \ldots$. In general the function $F(\omega)$ is a complex function of ω and to represent certain classes of signals $f(t)$, the integration must be carried out along a path in the complex ω plane. Numerical calculation of $F(\omega)$, given $f(t)$, can often be very time consuming even on a fast computer. However, most modern spectrum analyzers use a discrete version of the equation along with an efficient algorithm called the fast fourier transform (FFT). Given a set of data sampled at discrete time intervals

$\{f(t_k) = f_0, f_1, f_2, \ldots, f_k, \ldots f_N\}$, the discrete time FFT is defined by the formula

$$T(J) = \sum_{I=1}^{N} f(I)\, e^{-2\pi i (I-1)(J-1)/N}$$

where I and J are integers. Several points should be made here which may appear obvious. First, the signal $f(t)$ is time sampled at a fixed time interval τ_0 ; thus, information is lost for frequencies above $1/2\tau_0$. Second, only a finite set of points are used in the calculation, usually $N = 2^n$, and some built-in FFT electronics only for $N = 512$ or 1028 points. Thus information is lost about very low frequencies below $1/N\tau_0$. Finally the representation having no information about $F(t)$ before $t=t0$ or after $t = t_N$ essentially treats $f(t)$ as a periodic function. In general, this is not the case and since $f(t) \neq f(t_N)$, the Fourier representation treats this as a discontinuity which adds spurious information into $F(\omega)$. This is called the aliasing errors and methods exist to minimize its effect in $F(\omega)$

Hopkins et al [7] describe a method wherein the analysis of the spatial concentration field is carried out using a 3D fourier transform technique. The spatial concentration field is formed by dividing the control volume into cubical cells with a dimensionless width $a = w/d$, where d is the sphere diameter. The Fourier analysis is performed at regular intervals during the simulation. After each sphere is assigned to its respective cell in the grid, the concentration field is smoothed using a low pass filter. Using this smoothing function, a sphere in cell(i,j,k) contributes to the concentration in each grid cell. Finally the average concentration is subtracted from the concentration in each grid cell. The discrete Fourier transform of the smoothed concentration field minus its average value is calculated at regular intervals using a three-dimensional FFT algorithm. Hopkins et al. [7] state that the Fourier transform technique is particularly not practical for use over long periods of time. Thus although this method seems very well suited to the characterization of three dimensional flows, the efficiency of the method as a whole is not reasonable to warrant more work.

2.4 Variance Analysis Methods

An alternative to the FFT used by Sanders and Ackermann is to divide the control volume into uniform cells, count the number of particle centers in each cell and calculate the average variance of the concentration field. Hopkins et al[7] use such a method wherein, the cubical control volume is divided into a 10x10x10 array of cubical cells. The variance of the concentration field for a given realization of the system is

$$variance = (1/1000)\sum_{i}(n_i - N/1000)^2 \qquad (2.1)$$

where n_i is the number of sphere centers in each cell and N is the total number of spheres in the control volume. A series of experiments were performed with *6859* (19^3) spheres in which the coefficient of restitution was reduced from 0.9 to 0.2. The solid fraction υ was 0.2 and $L/d = 26$.

Although Hopkins et al[7] use a fixed grid size, it is questionable if the same results can be achieved with other grid sizes. We decided to investigate the effect of grid resolution upon the value of the variance and how it affects the correlation between the coefficient of restitution and the variance. A set of grid sizes were selected and the results

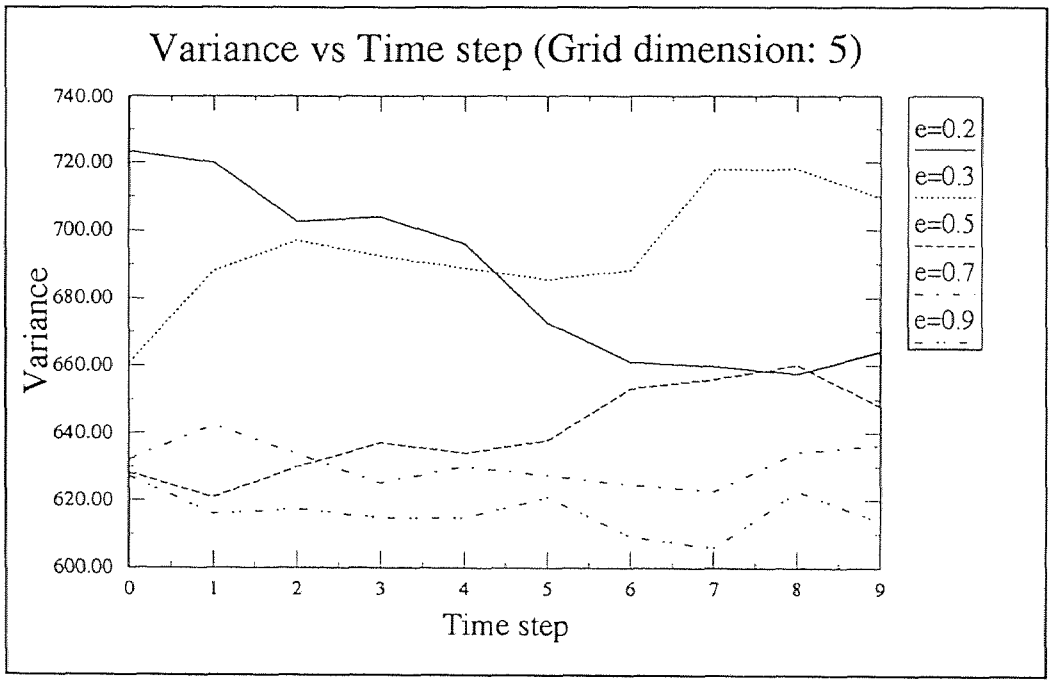

Figure 2.1 Variance versus time step for grid dimension of 5.

obtained. Figure 2.1 shows the results obtained for the case where the grid dimension was 5(In other words the volume is divided into 5x5x5 cubical array). Results obtained for other grid dimensions ranging from 10 through 25 appear in Appendix C. As the plots show, the variance analysis scheme's level of satisfactoriness seems to depend on the value chosen for the grid dimension. It appears that in this particular case, we may be able to achieve some degree of classification even with an arbitrary grid size, but it remains to be seen if the variance analysis method as described is as robust as other methods that are invariant to the classification method parameters for a given data analysis situation.

2.5 Geometric Methods

The intuitive evidence from two-dimensional slices of the three-dimensional shear flows showing homogeneous spatial regions of varying shape and size within the slice for various values of coefficient of restitution indicates that geometric methods in the plane could provide quantitative measures with which to characterize the microstructure present within. Among the geometric methods, we chose to focus our attention on methods that attack the problem of proximity, as the very nature of granular shear flows show some form of grouping of particles, thus suggesting the need for extracting the proximity information contained within. Preparata and Shamos[8] give an excellent description of fundamental algorithms that solve the proximity problem. As in most situations finding efficient algorithms for dimensions higher than two is fairly complex. As stated by Preparata and Shamos, "the status of this topic(proximity) of computational geometry is no exception to the by now familiar current standard: in the plane, powerful and elegant techniques are available while for the space - and even more in higher dimensions - very little is known and formidable difficulties lurk to suggest a negative prognosis". There exist several other geometrical objects that extract the properties of data in space such as the quadtree and octrees, but that do not really extract the proximity information. We use a single algorithm that discovers, processes, and stores compactly all of the relevant proximity information. To do this, we revive a classical mathematical object, the Voronoi diagram, and turn it into

an efficient computational structure that permits vast improvements over the best previously known algorithms. The Voronoi diagram, its properties and the application of the Voronoi diagram to the characterization of the microstructure in three-dimensional shear flows is discussed in detail in chapter 4.

Yet another intuitive understanding of the underlying structure as perceived visually can be realized through the use of fractals[6]. We could interpret the microstructure observable in two-dimensional slices of the three-dimensional shear flows as a being fractal in nature. The variegated pattern that can be seen can be given meaning through fractals. Fractals are basically sets that appear to have complex structure no matter what scale is used to examine them. One consequence of this definition is that true fractals must be infinite sets. Often, but not always, fractals have the same granularity across scales, so that one tends to see the same quality of structure in a fractal as one zooms in on it. Well behaved fractals such as these are the ones that have a well behaved fractal dimension. The fractal dimension is essentially an indication of how much space a given set comes near

CHAPTER 3
FRACTALS

3.1 Introduction

In three-dimensional shear flows, examination of two dimensional slices of the flow reveals a mazelike, multisheeted structure. This threadlike collection of points seems to have further structure when examined on a finer scale. To describe such variegations in the structure, we use the term fractal. An attempt is made in what follows to explain the meaning of fractals and how they may be used to characterize such patterned structures. A purely rigorous treatment may be found in Mandelbrot[9] and Falconer[10]. Two simple and popular examples are described below as an introduction to examples of fractal curves and sets.

3.1.1 Koch Curve:

The example is chosen from the book by Mandelbrot[9] and was originally described by Von Koch in 1904. One begins with a geometric construction that starts with a straight line segment of length 1. After dividing the line into three segments, one replaces the middle segment by two lines of length 1/3 as shown in figure3.1.Thus, we are left with four sides,

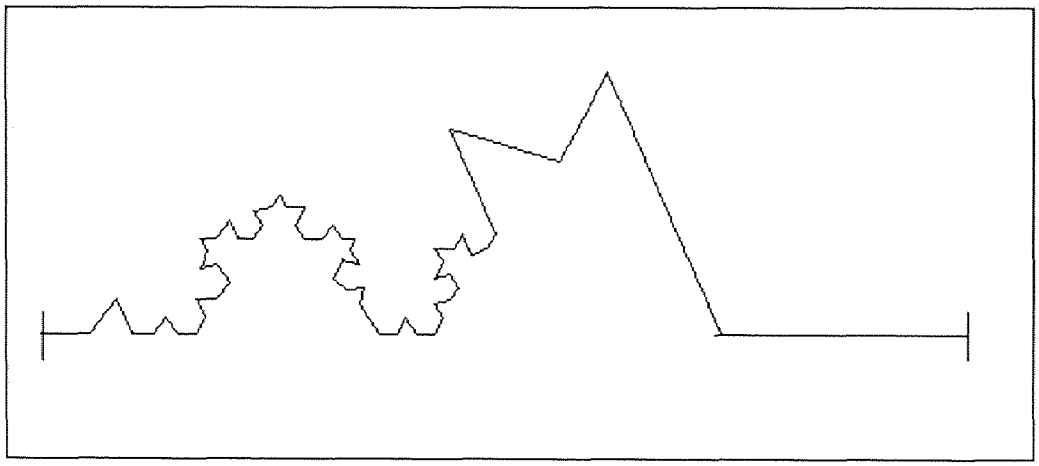

Figure 3.1 Partial construction of a fractal Koch curve.

each of length 1/3 so that the total length of the new boundary us 4/3. To get a fractal curve, one repeats this process for each of the new four segments and so on. At each step, the length is increased by 4/3 so that the total length approaches infinity.

After many steps, one can see that the curve looks fuzzy. In fact, the limit one has a continuous curve that is nowhere differentiable. In some sense, this new curve is trying to cover an area as a young child scribbling with crayons. Thus, we have the apparent paradox of a continuous curve that has some properties of an area. It is not surprising that one can define a dimension of this fractal curve which results in a value between 1 and 2.

3.1.2 Cantor Set:

The Cantor set is attributed to George Cantor (1845-1918), who discovered it in1883. If the Koch curve can be considered a process of adding finer and finer length structure to an initial line segment, then the Cantor set is the complement operation of removing smaller and smaller segments from a set of points initially from a line.

The construction begins as in the previous example with a line segment of length 1 which is subdivided into three sections as in figure 3.2. However, instead of adding two more segments as in the Koch curve, one removes the middle segment of points so that the total number of segments is increased to two, and the total length is reduced to 2/3. This

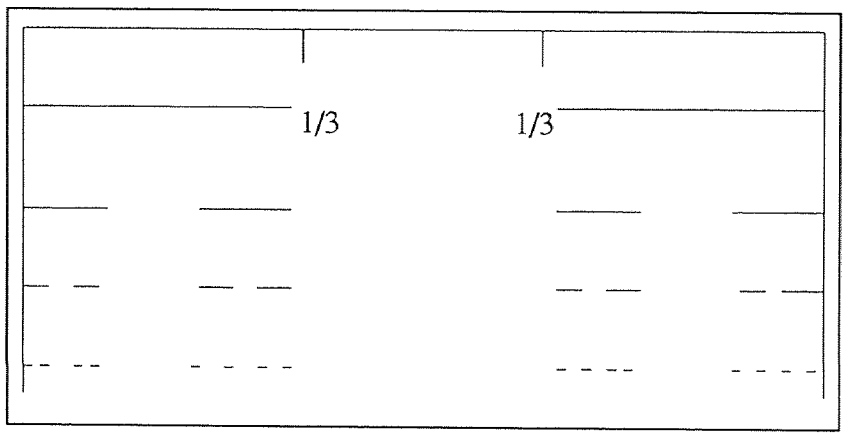

Figure 3.2 Top to bottom: sequential steps in the construction of a Cantor set.

process is continued for the remaining line segments and so on. At each stage one throws away the middle segments but reducing the total length by 2/3. In the limit, the total length approaches zero, although as we shall see below, the fractal dimension of this set of points is between zero and one.

3.2 Fractal Dimension

3.2.1 Meaning of Fractal Dimension

Fractal dimension could be described as a means of describing how much space a given set "comes near". For example a ball of twine appears 3-dimensional because it "comes near" enough the volume of a sphere to deceive our eyes. The Cantor set is another example, as described above, all its points lie on a straight line, but it is so full of gaps that no complete line segment, no matter how short, is contained in it. This is reflected in the fact that its fractal dimension is about 0.63. quite a bit less than 1.

Thus far we have two examples of fractal sets, but we do not have any test to determine if a set of points is fractal. There are many measures of the dimension of a set of points. We will describe a very intuitive or geometric definition called the capacity as described in Moon[6]. Other definitions which incorporate deeper mathematical subtleties, may be found in Mandelbrot[9] or Farmer et al. [11] as well as in the next section.

3.2.2 Pointwise Dimension

Let us consider a long time trajectory in phase space as shown in figure 3.1. First we sample the motion so that we have large number of points per orbit. Second, we place a sphere or cube of radius or length r at some point on the orbit and count the number of points within the sphere. The probability of finding a point in this sphere is then found by dividing by the total number of points in the orbit N_0; that is

$$P(r) = \frac{N(r)}{N_0}$$

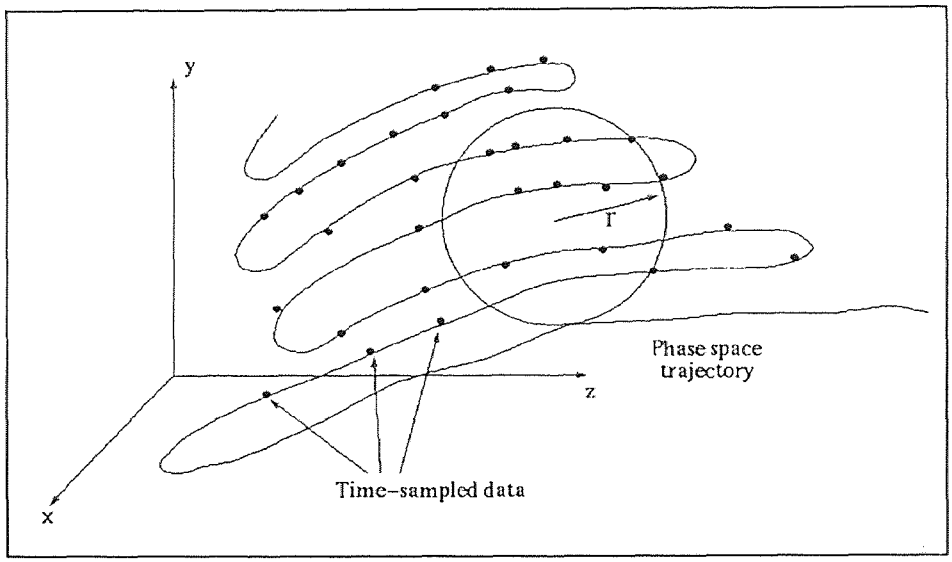

Figure 3.3 Long time trajectory of motion in phase space showing the time-sampled data points and the counting sphere.

For a one dimension orbit, such as a closed periodic orbit $P(r)$ will be linear in r as r->0, $N_0 \rightarrow \infty$; $P(r) = br$. If the orbit were quasiperiodic, for example, it lay on a two dimensional toroidal surface in three-dimensional

phase space, then the probability of finding a point on the orbit in a small

cube or sphere of radius r would be $P(r) = br^2$. This leads one to define a dimension of an orbit at a point x_i (there x_i is a vector in phase space) by measuring

the relative percentage of time that the orbit spends in the small sphere; that is

$$d_p = \lim_{r \to 0} \frac{\log P(r;x_i)}{\log r}$$

For some attractors, this definition will be independent of the point x_i. But for many, d_p will depend on x_i and an averaged pointwise dimension is best used. Also, for some sets of points such as a Cantor set, there will be gaps in the distribution of points so that $P(r)$ is not a smooth function of r as $r->0$, as can be seen.

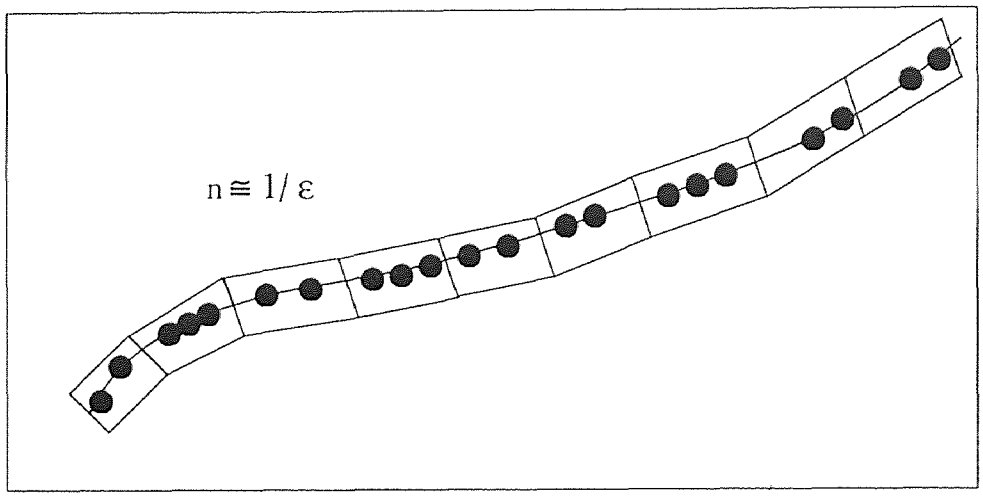

Figure 3.4 Covering procedure for linear distribution of points.

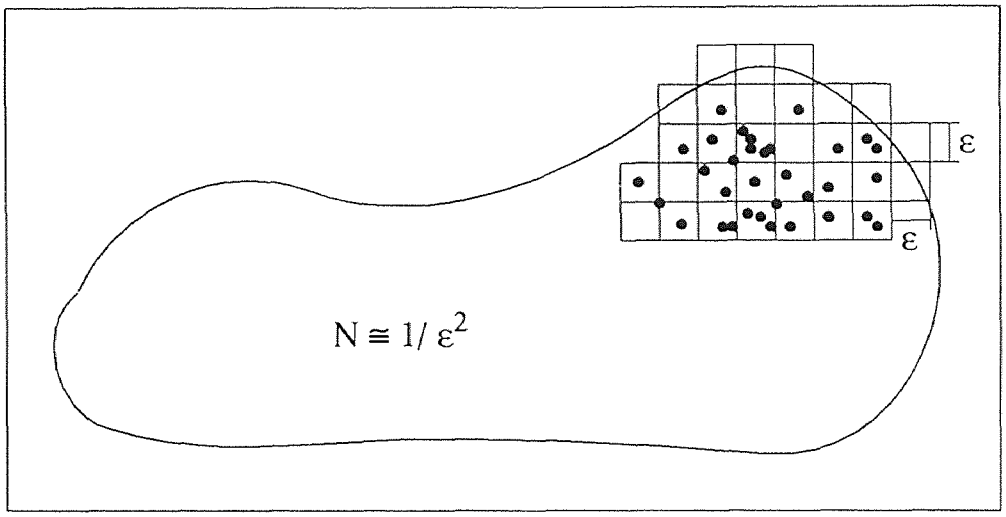

Figure 3.5 Covering procedure for planar distribution of points.

3.2.3 Capacity Dimension

First consider a uniform distribution of N_0 points along some line or one-dimensional manifold in a three-dimensional space, as shown in figure3.3. We then ask how we can cover this set of points with small cubes with sides of length ε. (one can also use spheres of radius ε.) To be more specific, we calculate the minimum number of such cubes $N(\varepsilon)$ to cover the set $(N(\varepsilon) < N_0)$. When N_0 is large, the number of cubes to cover aline will scale as

$$N(\varepsilon) = \frac{1}{\varepsilon}$$

Similarly, if we distribute points uniformly on some two-dimensional surface in three-dimensional space (see figure 3.4), we find that the minimum number (3.3) cover the set will scale in the following way.

$$N(\varepsilon) = \frac{1}{\varepsilon^2}$$

If the reader is convinced that this is intuitive, then it is natural to define the dimension followed by the following scaling law:

$$N(\varepsilon) = \frac{1}{\varepsilon^d}$$

Taking the logarithm of both sides of the equation above and adding a subscript to denote capacity dimension, we have

$$d_c = \lim_{\varepsilon \to 0} \frac{\log N(\varepsilon)}{\log (1/\varepsilon)}$$

Implicit in this definition is the requirement that the number of points in the set be large or N_0.

A set of points is said to be fractal if its dimension is noninteger - hence the term fractal dimension.

In the two examples of the Koch curve and the Cantor set, the fractal dimension can be calculated exactly. For example, consider the nth iteration of the generalization of the Koch curve where we let the size of the cubes be equal to the length of the straight line segment. At the nth step in the construction, the number of segments is

$$N_n = 4^n.$$

while the size ε is given

$$\varepsilon_n = (\frac{1}{3})^n$$

Replacing the limit ε->0 with $n \to \infty$ in equation one can easily see the Koch curve.

$$d_c = \frac{\log 4}{\log 3} = 1.26185\ldots$$

Similarly, one can show that for the cantor set

$$d = \frac{\log 2}{\log 3} \cong 0.63092\ldots$$

3.2.4 Correlation Dimension

This measure of fractal dimension has been used successfully by experimentalists and in some ways is related to the pointwise dimension. An extensive study of this definition of dimension has been given by Grassberger and Proccacia[12].

As in the definition of pointwise dimension, one discretizes the orbit to a set of N points $\{x_i\}$ in the phase space. (One can also create a pseudo-phase-space; One then calculates the distances between pairs of points, say $s_{ij} = | x_i - x_j |$ using either the conventional Euclidean measure of distance (square root of the sum of the squares of absolute value of vector components. A correlation function is then defined as

$$C(r) = \lim \frac{1}{N^2} \left(\begin{array}{c} number\ of\ pairs\ (i,j) \\ with\ distance\ s_{ij} < r \end{array} \right)$$

For many attractors this function has been found to exhibit a power law dependence on r as r -> 0; that is,

$$\lim_{r \to 0} C(r) = ar^d$$

so that one may define a fractal or correlation dimension using the slope of the ln C versus ln r curve:

$$d_G = \lim_{r \to 0} \frac{\log C(r)}{\log r}$$

It has been shown that $C(r)$ may be calculated more effectively by constructing a sphere or cube at each point x_i in phase space and counting the number of points in each

sphere; that is,

$$C(r) = \lim_{N\to\infty} \frac{1}{N^2} \sum_{i}^{N} \sum_{j}^{N} H(r - |x_i - x_j|)$$

where $H(s) = 1$ *if* $s > 0$ and $H(s) = 0$ *if* $s < 0$. This differs from the pointwise dimension in that the sum is performed about every point.

3.2.5 Information Dimension

Many investigators have suggested another definition of fractal dimension that is similar to the capacity but tries to account for the frequency with which the trajectory visits each covering cube. As in the definition of capacity, one covers the set of points, those dimension one wishes to measure, with a set of B cubes of s size e. This set of points is again a uniform discretization of the continuous trajectory. (It is assumes that a long enough trajectory is chosen to effectively cover the attractor whose dimension one wants to measure. For examples, if the motion s quasiperiodic, the trajectory has to long enough to "visit" all regions on the toroidal surface of the attractor.)

To calculate the information dimension, one count the number of points N_i in each of the N cells and the probability of finding a point in that cell P_i where

$$P \equiv \frac{N_i}{N_0}, \sum_{i}^{N} P_i = 1$$

where N_0 is the total number of points in the set. Note that $N_0 \neq N$

The information entropy is defined by the expression

$$I(\varepsilon) = -\sum_{i}^{N} P_i \log P_i$$

[when log function is with respect to base 2, I() has the units of bits].

For small ε, it is found that I behaves as,

$$I \cong d_I \log(1/\varepsilon)$$

so that for small ε we may define a dimension

$$d_I = \lim_{\varepsilon \to 0} \frac{I(\varepsilon)}{\log(1/\varepsilon)} = \lim_{\varepsilon \to 0} \frac{\sum P_i \log P_i}{\log \varepsilon}$$

To see that this definition is related to the capacity, we note that if the probabilities P_i are equal for all cells, that is.

$$P = \frac{N_i}{N_0} = \frac{1}{N}$$

then

$$I = \sum P_i \log P_i = -\frac{1}{N} \log \frac{1}{N} = \log N$$

The information entropy is a measure of the unpredictability in a system. That is, for a uniform probability in each cell, $N_i = 1/N$, I is at a maximum. If all the points are located in one cell(maximum predictability) I = 0, as can be seen from the calculation.

3.2.6 Properties of Fractal Dimension

We can list the following properties of the fractal dimension:

1. The fractal dimension describes how many new pieces of a set are resolved as the resolution scale is decreased.

2. As fractals are self-similar, it follows that the fractal dimension can be evaluated by comparing properties between any two scales.

3.3 Application of Fractal Dimension

3.3.1 Introduction

We have seen that there are several measures of the fractal dimension. We make use of the capacity, the information and the correlation dimensions. It would seem that the capacity dimension would intuitively provide us with the information contained in the microstructure. But, there are two criticisms of the use of capacity as measure of fractal dimension of strange attractors. - one theoretical and the other computational. First,

capacity dimension is a geometric measure; that is, it does not account for the frequency with which the orbit might visit the covering cube or ball. Second the process of counting a covering set of hypercubes in phase space is very time consuming computationally. We use the method described in Liebovitch and Toth[13] to determine the fractal dimension by box counting or the method for capacity dimension. The method they describe is fast, accurate and less dependent on data specific curve fitting criteria than the correlation dimension.

3.3.2 Computation of the box dimension.

To compute the box dimension[13], we need to count the number of boxes in a minimal cover that contain at least one element of the set. This is then carried out for a sequence of decreasing box sizes. The algorithm used does this by an efficient hashing to code all the points within one box with the same number and then to count the number of distinct values. Each of the N points of a set embedded in d_e dimensions can be represented by a vector with coordinates $\{ X_i; i = 1, d_e \}$. The values of X_i are normalized to cover the range $(0, 2^{k-1})$. The set is covered by a grid of d_e dimensional cubes of edge size $2m$, $0<=m<=k$, called boxes. For each coordinate we form $Y_i = (X_i \; AND \; M)$ where AND is the binary construction of the corresponding bits in X_i and M, and M is a binary number with 1's in the first k-m places and 0's the remainder. Then for each $n = 1,..., N$ we construct $Z_n = Y_1+Y_2+Y_3+...+Y_{de}$, where the operation "+" indicates concatenation (for example, "10+01" = "1001"). All the points within the same box of size $2m$ will have coordinates that have identical binary digits in the first k- m places. Thus, distinct Z_n correspond to points in distinct boxes. The number of distinct Z_n is counted in an efficient manner by ordering them using a quicksort or heapsort to order all N strings Z_n, and then walk down the list once to count the number of times the value change. The procedure is then repeated for . different boxes of edge size $2m$, where $m = k, k-1,..., 0$

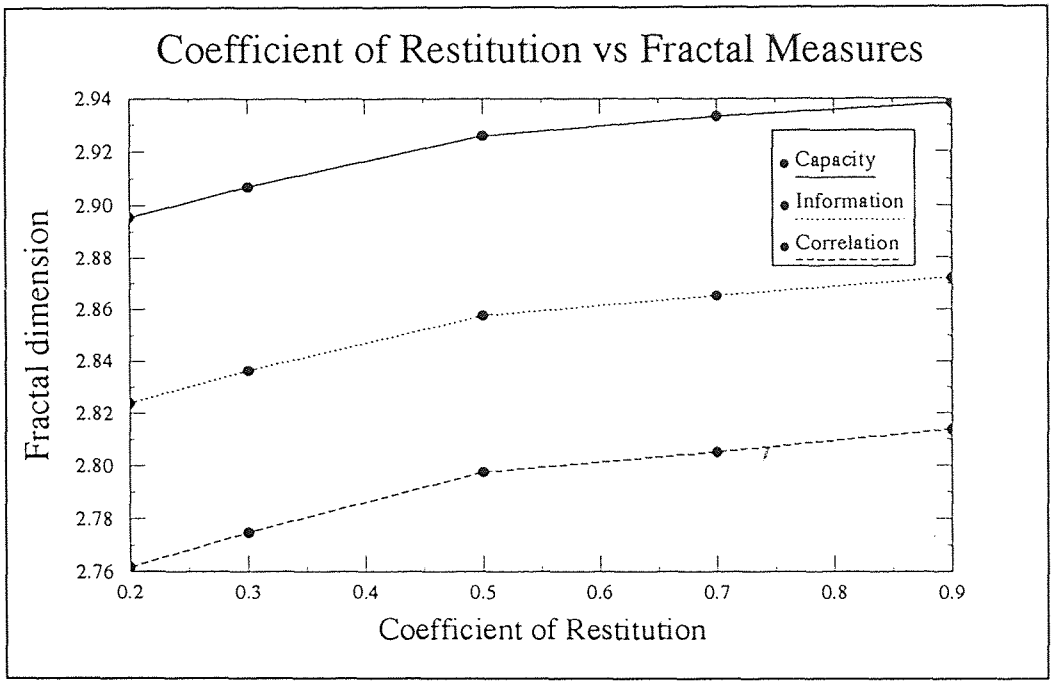

Figure 3.6 Coefficient of Restitution versus Fractal Measures

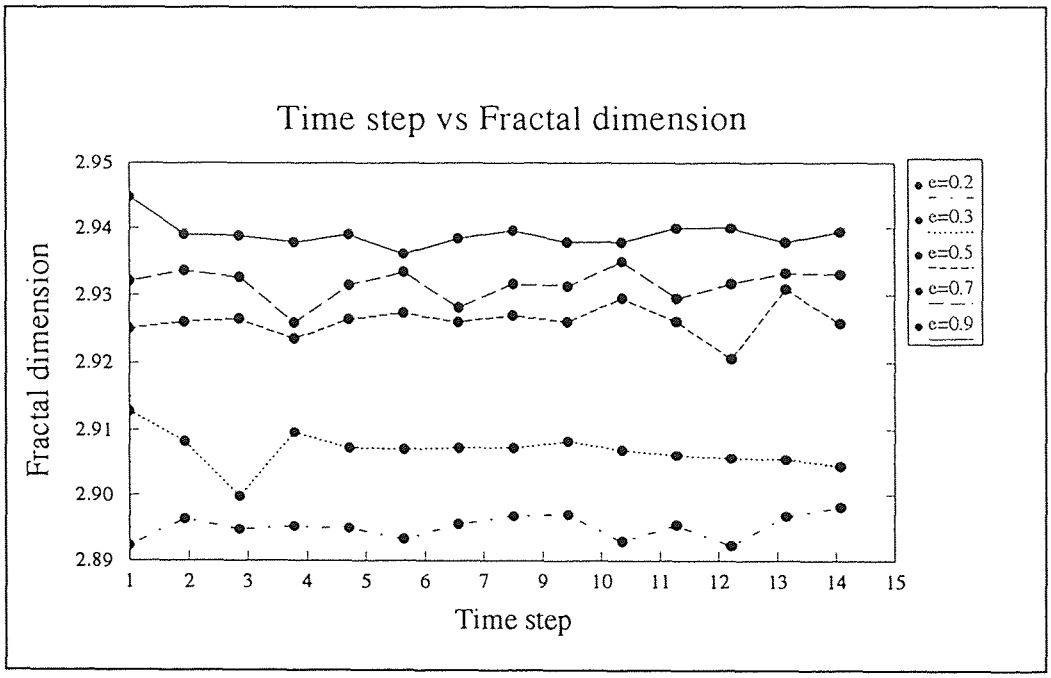

Figure 3.7 Time step versus Fractal dimension

3.4 Results

The code made available by Prof. John Sarraille of Computer Science Dept., CSU Stanislaus, CA was used to extract measures of the fractal dimension. Figure 3.6 shows the plot of the coefficient of restitution versus the fractal dimension. As can be seen, each of the three measures *viz.*, the capacity dimension, the information dimension and the correlation dimension, has a different value for a specific value of the coefficient of restitution, but they all have the same trend thus indicating a well behaved fractal dimension. Figure 3.7 shows the plot of the fractal dimension for various time steps for different values of coefficient of restitution. As with the results obtained with the variance analysis scheme, these results clearly indicate the presence of a microstructure for different values of the coefficient of restitution, but the demarcation is improved and is independent of any artifacts of the method.

3.5 Conclusion

The fractal dimension used to characterize the structure in three-dimensional shear flows has been shown to be successful. Thus it would seem reasonable to infer that the fractal dimension is superior to other methods in several ways. The fractal dimension is fixed at any resolution as a result of the self similarity property of fractals. Fractals have the same granularity across scales, or are even self-similar across scales, so that one tends to see the same quality of structure as one zooms in on it. The fractal dimension is also independent of any parameters and in this respect it is better than the measure obtained through the variance analysis scheme. In summary, the fractal dimension as a classification tool holds great promise because it is relatively easy to estimate the fractal dimension of a set S, because we know that a chaotic system gave rise to the set S if this dimension is not an integer, and because the value of the dimension gives us some indication of what type of chaotic system gave rise to S.

CHAPTER 4
VORONOI DIAGRAM

4.1 Introduction

The microstructure to be found in three dimensional shear flows has been confirmed by other researchers[7] to have a distinct structure at low coefficients of restitution, where the formation of closely grouped aggregations dominate. The gestaltic nature of such microstructure indicates that an approach that extracts the proximity information contained within could classify variations in such structure based on the properties relating to proximity. After surveying various algorithms for the proximity problem in computational geometry, we choose to use the Voronoi diagram[14] as it relates most to the task on hand.

4.2 Voronoi Diagrams

4.2.1 Loci of proximity

The problem can be expressed as follows: Given a set S of N points in the plane, for each point p_i in S what is the locus of points (x, y) in the plane that are closer to pi than to any other point in S.

Note that intuitively, the solution to the above problem is a partition of the plane into regions (each region being the locus of the points (x, y) closer to a point S than to any other point of S). We also note that, if we know this partition, by searching it(i.e., by locating a query point q in the region of this partition), we could directly solve the nearest neighbor search problem. We shall now analyze the structure of the partition of the plane. Given two points, p_i and p_j, the set of points closer to pi than to p_j is just the half-plane containing p_i that is defined by the perpendicular bisector of $\overline{p_i}\overline{p_j}$. Let us denote the half-plane by $H(p_i, p_j)$. The locus of points closer to p_j than to any other point, which we denote by $V(i)$, is the intersection of $N-1$ half planes, and is convex polygonal region having no more than $N-1$ sides that is

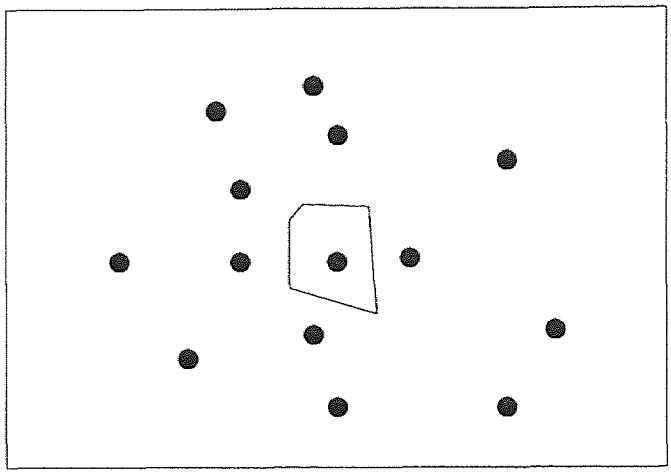

Figure 4.1 A Voronoi polygon.

$V(i)$ is called the Voronoi Polygon associated with p_i. A voronoi polygon is shown in Figure 4.1. These N regions partition the plane into a convex net which we shall refer to as the Voronoi diagram, denoted as Vor(S), which is shown in Figure 4.1. The vertices of the Voronoi diagram are the Voronoi Vertices, and its line segments are Voronoi edges. Each of the original N points belongs to a unique Voronoi polygon; thus if$(x, y) \in V(i)$, then p_i is a nearest neighbor of (x, y). the Voronoi diagram contains in a powerful sense, all of the proximity information defined by the given set.

4.2.2 Construction of the Voronoi Diagram

By constructing the Voronoi Diagram Vor(S) of a set of points S, we shall mean to produce a formal description of the diagram as a planar graph embedded in the plane consisting of the following items.

1. The coordinates of the Voronoi vertices.

2. The set of edges (each as a pair of Voronoi vertices) and the two edges that are their counterclockwise successors at each extreme point (doubly connected-edge-list, see Appendix B). This implicitly provides the counterclockwise edge cycle at each vertex and the clockwise edge cycle. We consider first the question of time necessary for constructing

the Voronoi diagram. We assume now, and later substantiate, that in any case Step *1* can be carried out in time *O(N)*. If we let *T(N)* denote the overall running time of the algorithm, then Step *2* is completed in time approximately *2T(N/2)*. Thus, if Vor(*S1*) and Vor(*S2*) can be merged in linear time to form the Voronoi diagram Vor(*S*) of the entire set, we will have a $\theta(N\log N)$ optimal algorithm.

Step *1*. Partition *S* into two subsets *S1* and *S2*, of approximately equal sizes, by median *x*-coordinate.

Step *2*. Construct Vor(*S1*) and Vor(*S2*) recursively.

Step *3'*. Construct the polygonal chain *SIGMA*, separating *S1* and *S2*.

Step *3"*. Discard all edges of Vor(*S2*) that lie to the left of *SIGMA* and all edges of Vor(*S1*) that lie to the right of *SIGMA*. The result is Vor(*S*), the Voronoi diagram of the entire set.

Clearly their success of this procedure depends on how rapidly we are able to construct *SIGMA*, since Step *3"* poses no difficulties.

From a performance viewpoint, the initial partition of *S* according to the median of the x-coordinates can be done in O(*N*) by standard median finding algorithms. Moreover, Step *3"* can be carried out in time $O(|S1| + |S2|) = O(N)$.

4.2.3 Constructing the dividing chain.

The first step in the construction of *SIGMA* is to find its semi-infinite rays. We observe that each ray of *SIGMA* is the perpendicular of a supporting segment of *CH(S1)* and *CH(S2)*. We also note that, since *S1* and *S2* are linearly separated by hypothesis, there are just two supporting segments of *CH(S1)* and *CH(S2)*(thereby confirming that *SIGMA*(*S1*, *S2*) consists of just one chain *SIGMA*). If we now assume inductively that these two convex hulls are available, their two supporting segments, denoted *t1* and *t2*, are constructed in (at most) linear time[15] and the rays of *SIGMA* are readily determined (see Figure 4.2). Notice that as a by-product of this activity we also obtain *CH(S)*, thereby providing the induction step for the availability of the convex hulls. Once we have found a ray of

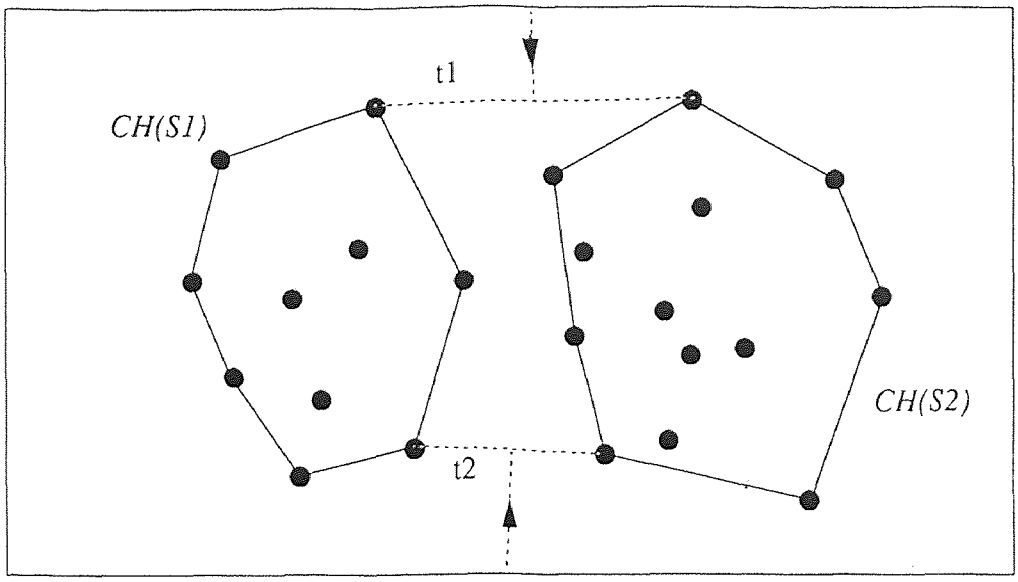

Figure 4.2 Finding the rays of SIGMA, the dividing chain.

SIGMA, the construction continues edge by edge, until the other ray is reached.

The time required by the recursive merge procedure is described by the recurrence relation $T(N) = 2T(N/2) + O(N) = O(NlogN)$.

4.3 Application of Voronoi Diagram

4.3.1 Geometrical measures of Voronoi primitives

There are several measures that can be extracted from the Voronoi diagram primitives as discussed by Ahuja[16]. Examples of some joint properties that may be useful are: distance between neighbors, gradients of primitive features, and status of neighbors with respect to completeness of cells. Sibson[17] has suggested the use of areas and nucleus-vertex distances of Voronoi polygons and the distances between neighboring points as statistics of a point pattern. For the microstructure contained in two dimensional slices of the three dimensional shear flows, we employ the following measures:

1. Areas of the Voronoi Polygons and their inverses.

2. Areas of the Delaunay triangles and their inverses.

3. Edge lengths of the Delaunay triangles.

We choose these measures over other neighborhood properties as they succinctly summarize the information relating to the structure between varying values of e.

4.3.2 Classification based on statistical measures

The classification scheme used here is based on identifying first and second order statistics relating to the measures outlined in 4.3.1. A histogram plot of these measures is taken to describe the distribution of the measures for a given structure. Figure 4.3 shows the data and the corresponding Voronoi diagram and Delaunay triangulation for the two extreme cases viz., e=0.2 and e=0.9. Table 4.1 summarizes the results of the classification scheme. Appendix D contains the plots describing the mean, the standard deviation, the median and the covariance of the various measures considered. The plots shown are taken from the data resulting from the two extreme cases *viz.*, for the coefficient of restitution of 0.2 where there exists a distinct structure and that for which the structure is less distinct.

4.4 Results

4.4.1 Evaluation of results

The data shown in Figure 4.3 clearly is not readily perceivable as being different, yet the Voronoi diagram and Delaunay triangulations as seen in the figure, elicit the presence of structure. From Table 4.1, it can be seen from the numerical values that the scheme outlined above has been successful as is indicated by the variation among the statistical measures for the various plots between the two extreme cases

Table 4.1 Summary of Results for Statistical Parameters from the Voronoi Diagram

Coefficient of Restitution	Polygon Areas Mean	Triangle Areas Mean	Triangle Lengths Mean
0.2	32.0	7.6	4.8
0.9	36.0	8.3	5.2

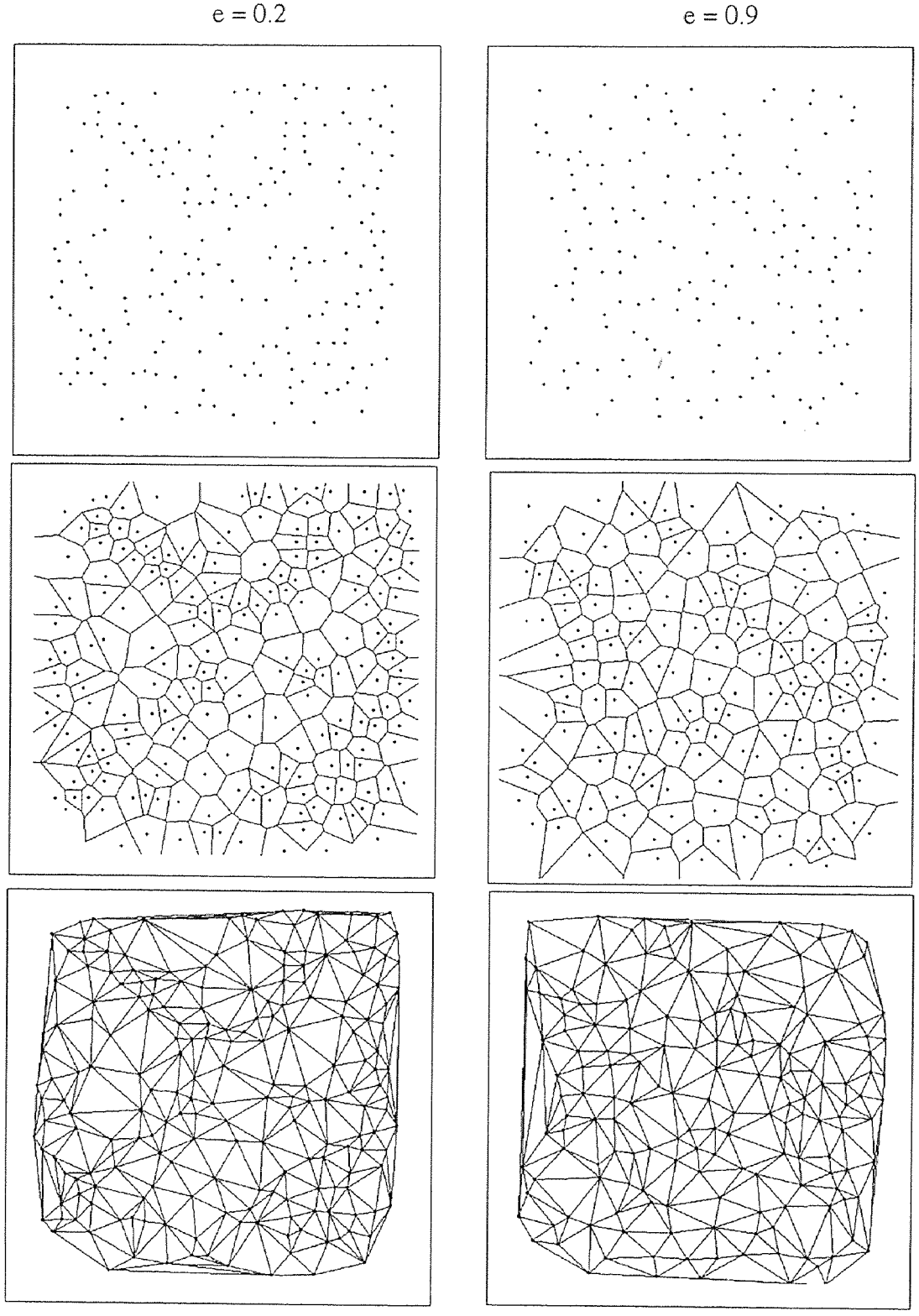

Figure 4.3 Two dimensional slice data, their corresponding Voronoi diagrams and Delaunay triangulations.

4.4.2 Limitations

The measures we have utilized have been shown to work, but the scale of separation indicates that they need further refinement to be able to produce a more nuanced discrimination between microstructures. Thus these methods are satisfactory for the data presented here, but would need to employ a classification scheme that can identify aggregate properties to better distinguish between microstructures. It should also be pointed out however, that as a result of the parameters in the data generation code[5], the data used in this work has a minor gradation in the structure from e=0.2 to e=0.9 compared to the marked gradation reported by other researchers.

4.5 Conclusions

The measures introduced based on the extraction of properties relating to the proximity have been shown to be satisfactory. The Voronoi diagram and the Delaunay triangulations are indeed powerful geometric objects as applicable to the characterization of microstructure in three dimensional shear flows. However, the scheme introduced here would be particularly effective for data that has a clear gradation between the structures as reported by other researchers. The method introduced here has provided insight into how it may be better adapted to provide a more discriminatory classification and may also be used as a front-end for other schemes.

CHAPTER 5
CONCLUSION

The goal of this thesis has been to investigate new methods to characterize the structure present in three-dimensional shear flows and address the problems faced by methods used in the past and to solve to some extent the problems faced by them. To this end, the methods introduced have been shown to be successful. The methods are efficient, robust and independent of any parameters of classification unlike the variance analysis method that seems to have questionable results with varying grid dimension.

The extraction of the fractal dimension of the microstructure and the existence of distinct values for different coefficients of restitution indicates that this approach is particularly useful and could be used as a front end in future research for further refinement of the classification scheme for the problem. The statistical measures formed from the geometric properties of the Voronoi diagram viz., the Delaunay edge lengths, the Voronoi polygon areas and the perimeters of the Voronoi polygon and Delaunay triangles have been to shown to work even in the case of marginal microstructure, thus indicating that future research can be directed towards employing the Voronoi diagram in aggregating group properties of characteristic regions of the microstructure.

In summary two new methods have been introduced that have been shown to be successful. The new methods introduced are independent of the parameters of classification and are computationally efficient ($O(NlogN)$) and fairly robust. These methods can be used as a front end for improving the classification scheme and could be easily extended to other data analysis situations of a similar nature.

APPENDIX A

OBJECT ORIENTED DESIGN

Object-orientation[18] is a way of thinking, not tied to any particular language, merely a mindset which is itself supported better by more recent languages. The object oriented paradigm, at its simplest, takes the standard components of any software system - data and procedures - but de-emphasizing the procedures, stressing instead the encapsulation, in an autonomous module of data and procedural features together, exemplified by the clear and concise specification of the module interface. In a systems decomposition based on an object oriented approach, the system is viewed as a collection of objects, sometimes referred to as entities. High level analysis and design is accomplished not only in terms of these objects but also in terms of the ways in which objects interact with each other via "messages" that pass information, invoking the objects to implement a procedures "behavior") or to reply with details about its state.

Detailed design, including procedure implementation and specification of data-structures is deferred until much later in the development process and implementation details are generally private to the object, the "visible" characteristics being strictly limited and tightly controlled, thus adhering strictly to the concepts of information hiding as promulgated by Parnas. Consequently, algorithmic procedures and data structures are no longer "frozen" at a high level of system design. A system based upon object representation can remain more flexible since changes at the implementation level are more easily accomplished since implementation details tend to be hidden and therefore changes have highly limited impact on other parts of the program. It is important that data structures provide the basis of object identification around which an interface is then developed. Thus object development focuses on data abstraction rather than freezing specific data structures into object specification.

In contrast to the common structured systems analysis, based largely on top-down functional decomposition, object oriented(OO) design and analysis has many attributes of both top-down and, perhaps pre-dominantly, bottom up design. Since one of the aims of an OO implementation is the development of generic classes for storage in libraries (the software engineering "holy grail"of the reusability), an approach that considers both top-down analysis and bottom-up design simultaneously is likely to lead to the most robust software systems

Indeed several authors suggest that in reality, practitioners purporting to be following a strictly top-down apporach actually utilize a mixed mode of operation between top-down,, bottom-up, and middle-out.

Since a significant portion of object oriented systems development is bottom up, the differentiation between program design and coding is much less distinct than in a procedurally based systems life cycle. However, at this,later stage, it would seem reasonable that within individual code modules the tools developed for high level functional decomposition and top-down system design such as DFDs, can still be found to be useful. Other graphical tools that are useful at different stages within OO systems life cycle and object relationship graphs, client server diagrams, object design diagrams, class interface diagrams, inheritance charts, or collaboration graphs.

APPENDIX B

THE DOUBLY CONNECTED EDGE LIST(DCEL)

The doubly-connected edge-list (DCEL) as described in Preparata and Shamos[] is particularly suited to represent a planar graph embedded in the plane. A planar embedding of a planar graph G = (V, E) is the mapping of each vertex in V to a point in the plane and each edge in E to a simple curve between the two images of extreme vertices of the edge, so that no two images of edges intersect except at the endpoints.

Let V = $\{v_1,..., v_N\}$ and E = $\{e_1,..., e_M\}$. The main component of the DCEL of a planar graph (V, E) is the edge node. There is a one-to-one correspondence between edges and edge nodes, i.e., each edge is represented exactly once. An edge node consists of four information fields V1, V2, F1 and F2, and two pointer fields P1 and P2: therefore the corresponding data structure is easily implemented with six arrays with the same names, each consisting of M cells. The meanings of these fields are as follows. The field V1 contains the origin of the edge and the field V2 contains its terminus; in this manner the edge receives a conventional orientation. the fields F1 and F2 of the edge oriented from V1 to V2. The pointer P1(resp. P2) points to the edge node containing the first edge encountered after the edge(V1, V2) when one proceeds counterclockwise around V1(resp. V2). Names

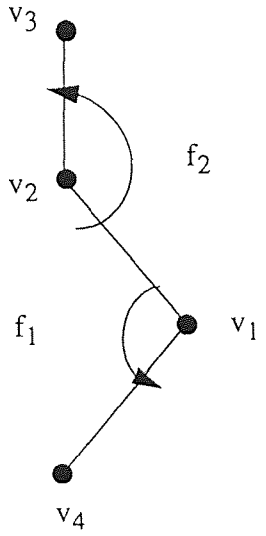

	V1	V2	F1	F2	P1	P2
1						
2						
a1	1	2	1	2	a2	a3
a2	4	1	1			
a3	2	3		2		

Figure B1 Doubly connected edge list

of faces and vertices may be taken as integers. As an example, a fragment of a graph and the corresponding fragment of the DCEL are shown in the figure below.

It is now easy to see how the edges incident on a given vertex or the edges enclosing a given face can be obtained from the DCEL. If the graph has N vertices and F faces, we can assume we have two arrays HV[1:N] and HF[1:F] of headers of the vertex and face lists: these arrays can be filled by a scan of arrays V1 and F1 in time O(N). The following straightforward procedure VERTEX(j), obtains the sequence of edges incident on v_j as a sequence of addresses stored in an array A.

```
procedure VERTEX(j)
begin a:= HV[j];
        a0:= a;
        A[1]:= a;
        i:=2;
        if(V1[a] = j)then a:= P1[a] else a:= P2[a];
        while(a != a0) do
                begin A[i]:= a;
                        if(V1[a] = j) then a:= P1[a] else a:= P2[a];
                        i:= i + 1
                end
end
```

Clearly VERTEX(j) runs in time proportional to the number of edges incident on v_j. Analogously, we can develop a procedure, FACE(j), which obtains the sequence of edges enclosing f_j, by replacing HV and V1 with HF and F1, respectively, in the above procedure VERTEX(j). Notice that the procedure VERTEX traces the edges counterclockwise about a vertex while FACE traces then clockwise about a face.

APPENDIX C

VARIANCE ANALYSIS PLOTS

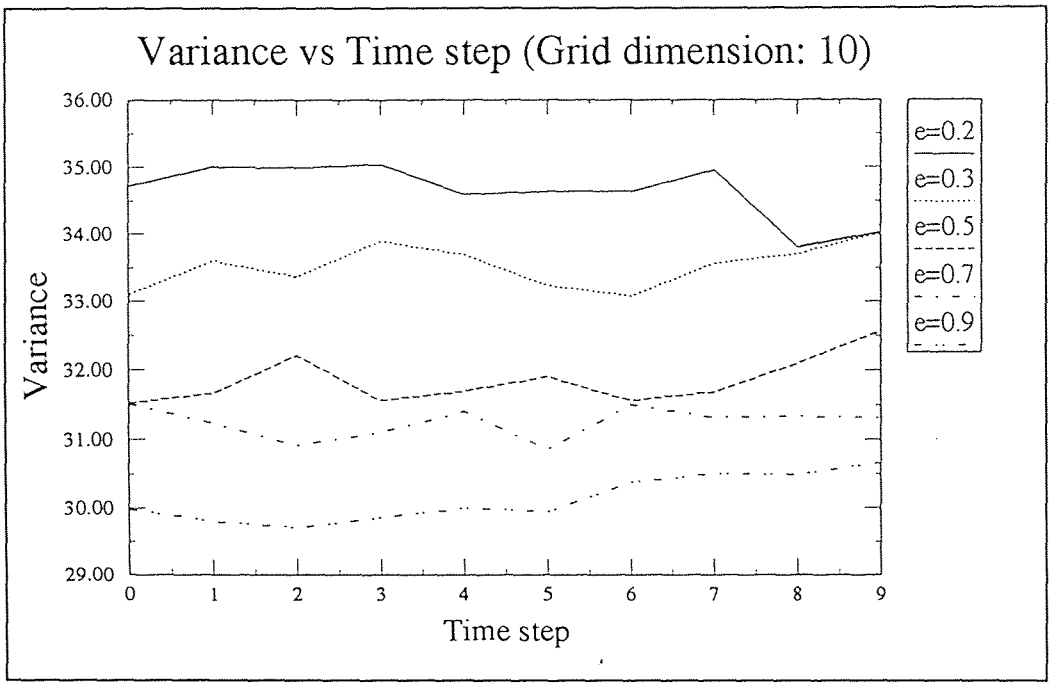

Figure C1 Variance versus Time step for grid dimension of 10

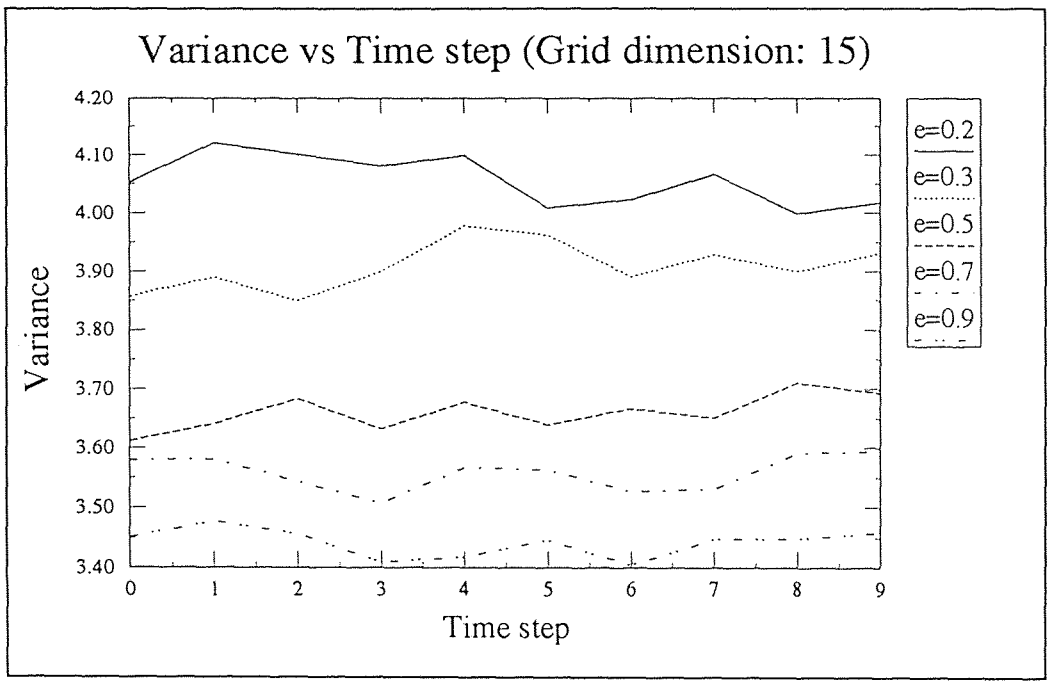

Figure C2 Variance versus Time step for grid dimension of 15

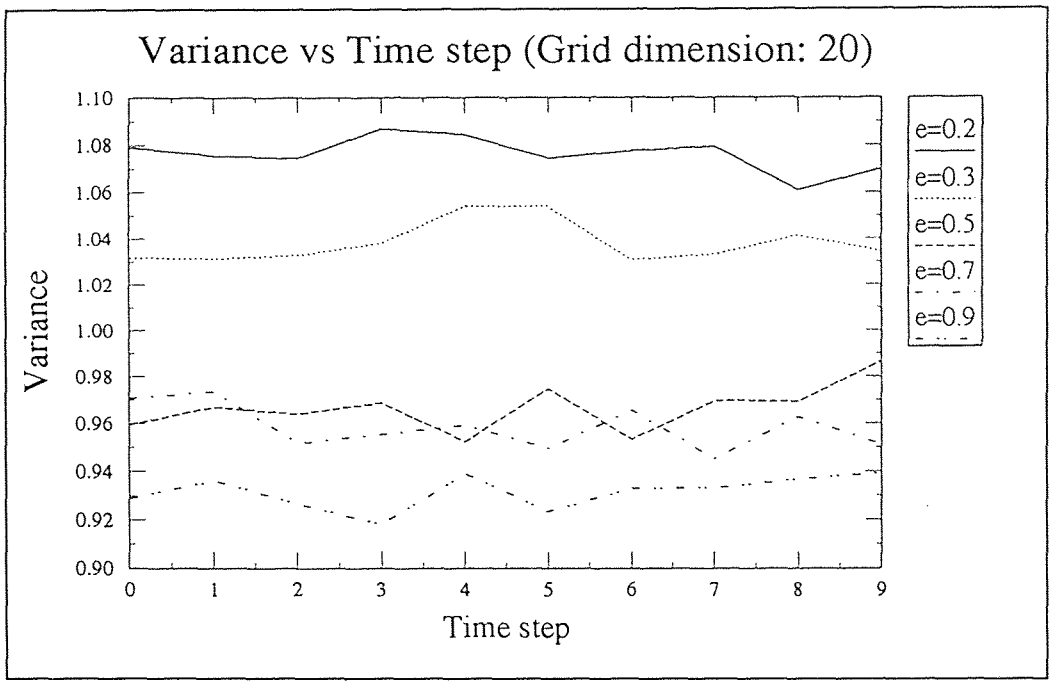

Figure C3 Variance versus Time step for grid dimension of 20

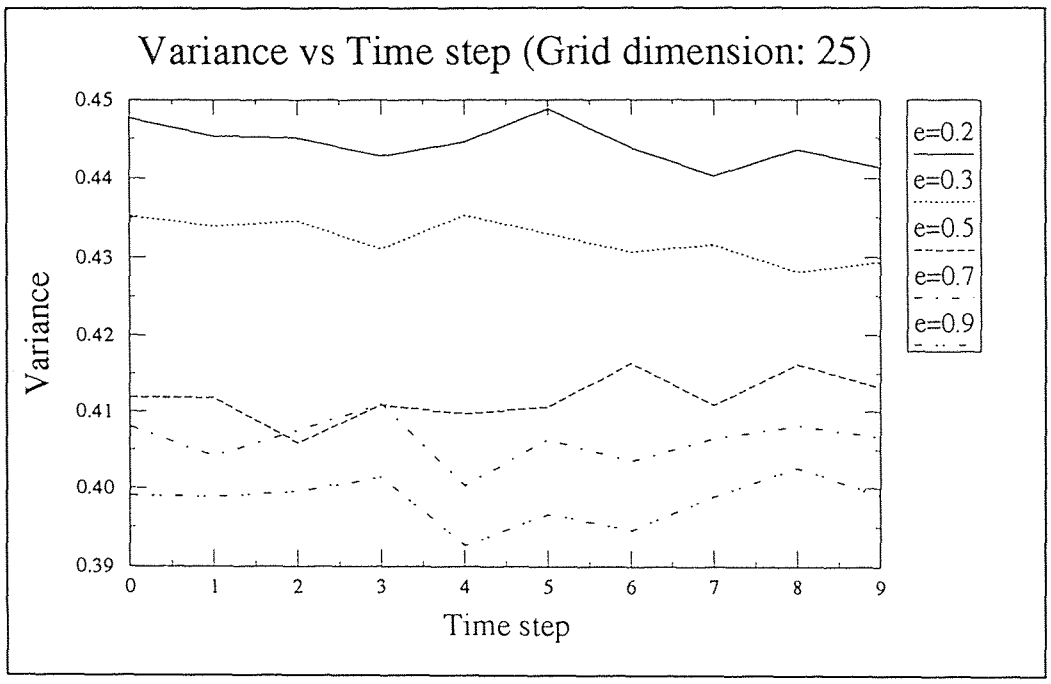

Figure C4 Variance versus Time step for grid dimension of 25

APPENDIX D

HISTOGRAM PLOTS OF VORONOI DIAGRAM MEASURES

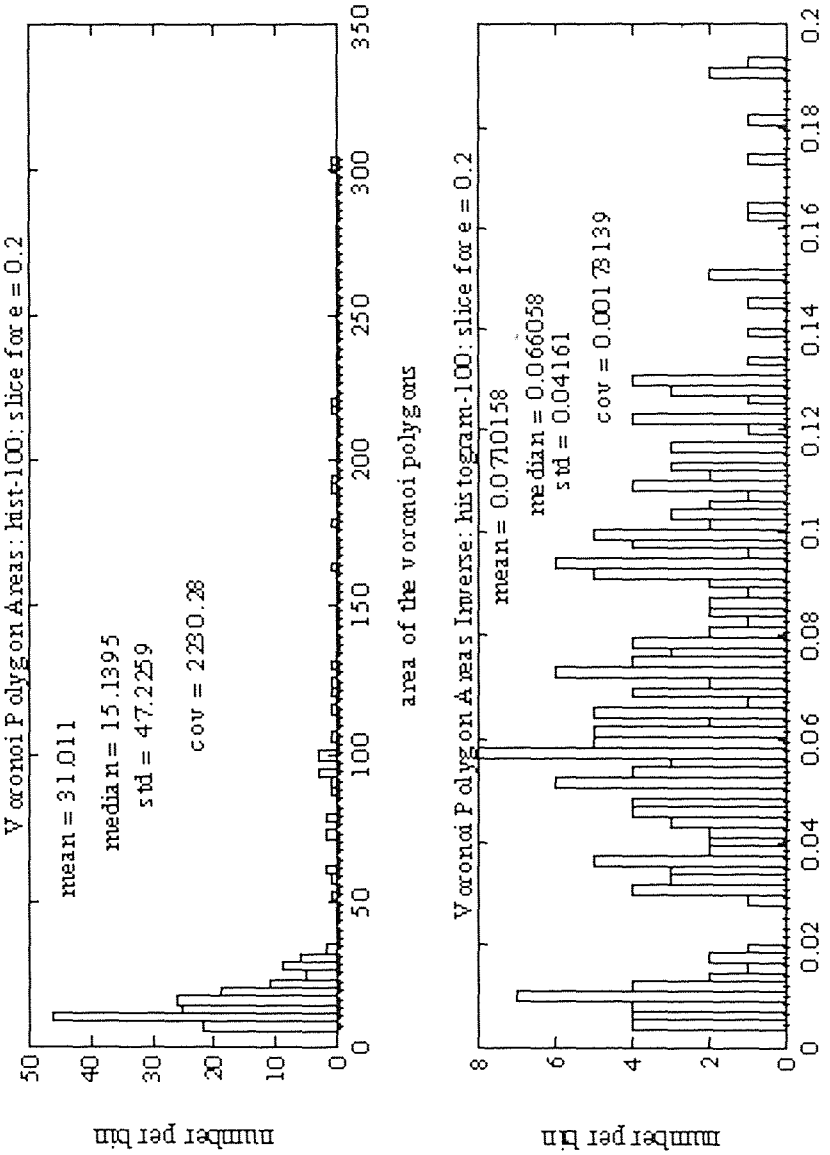

Figure D1 Histogram plot for Voronoi Polygon areas and their inverses for e=0.2

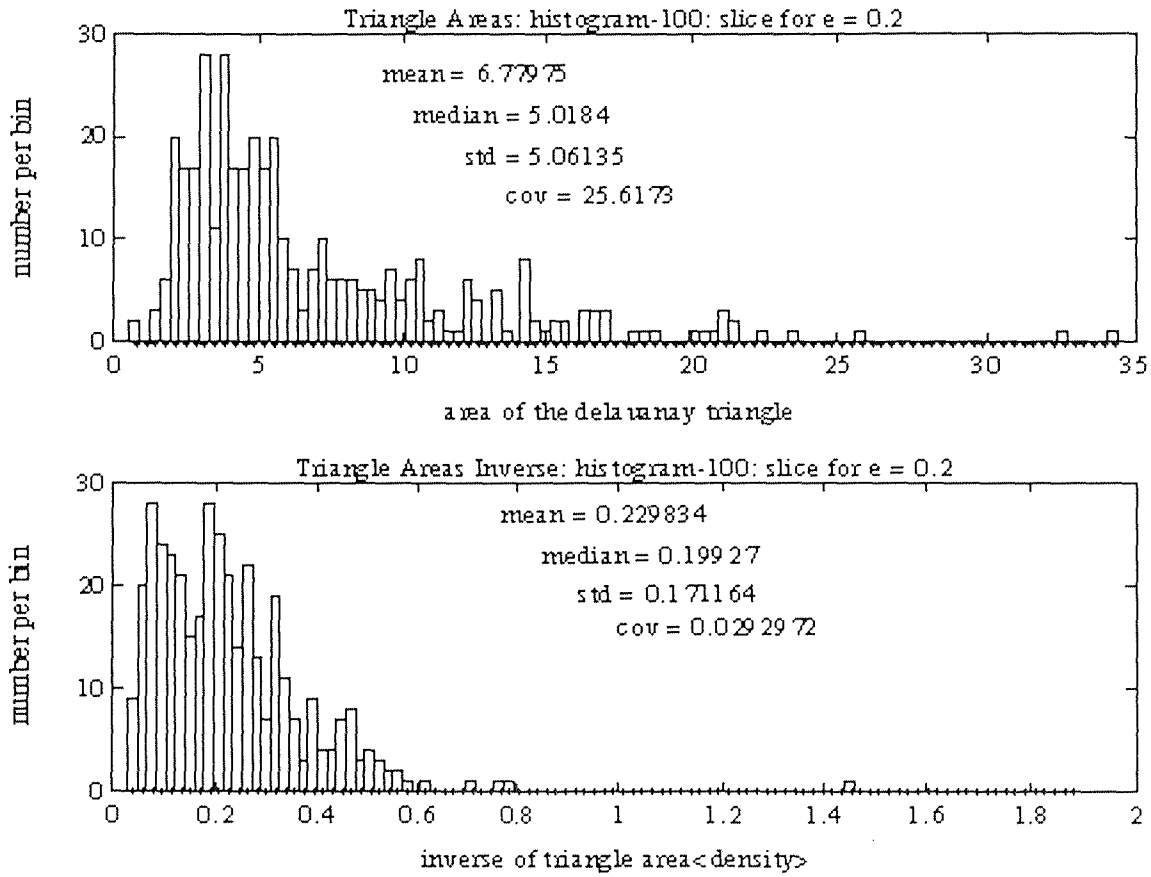

Figure D2 Histogram plot for Delaunay triangle areas and their inverses for e=0.2

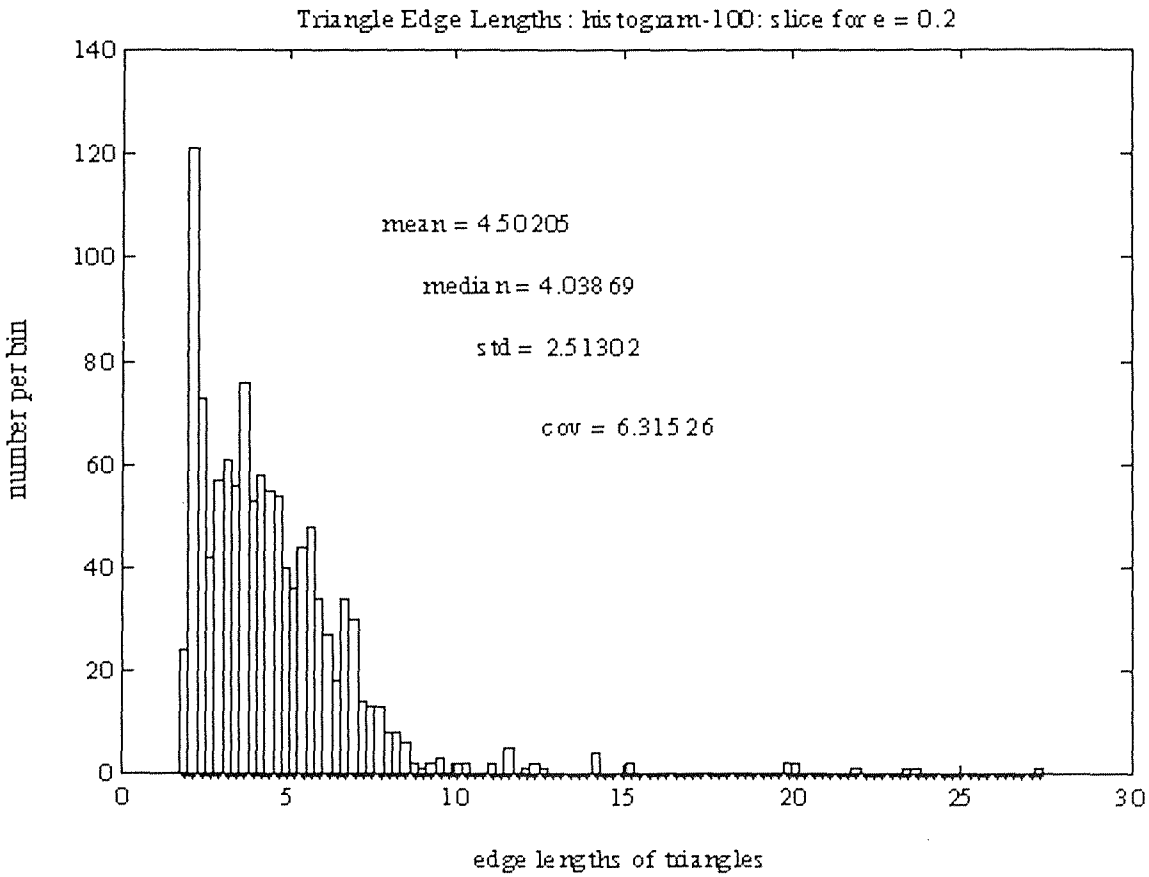

Figure D3 Histogram plot for Delaunay triangle edge lengths for e=0.2

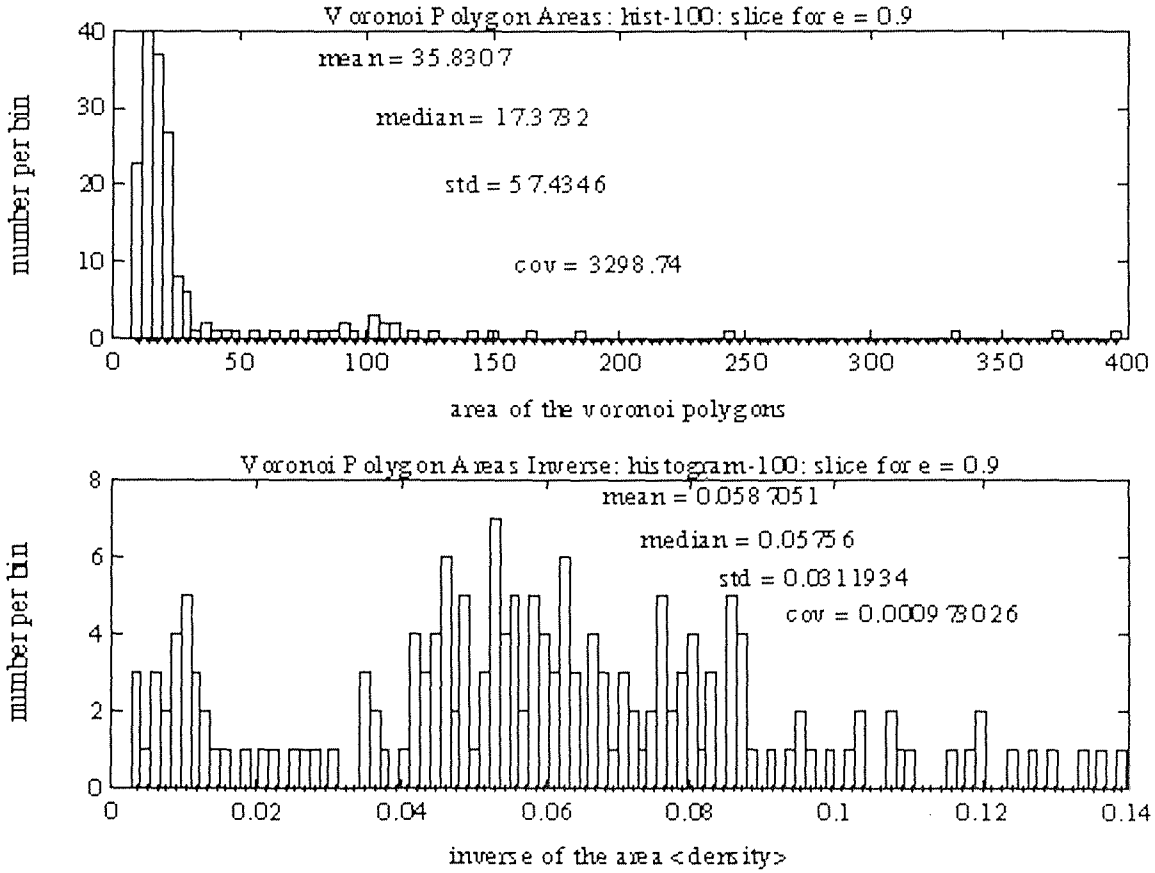

Figure D4 Histogram plot for Voronoi polygon areas and their inverses for e=0.9

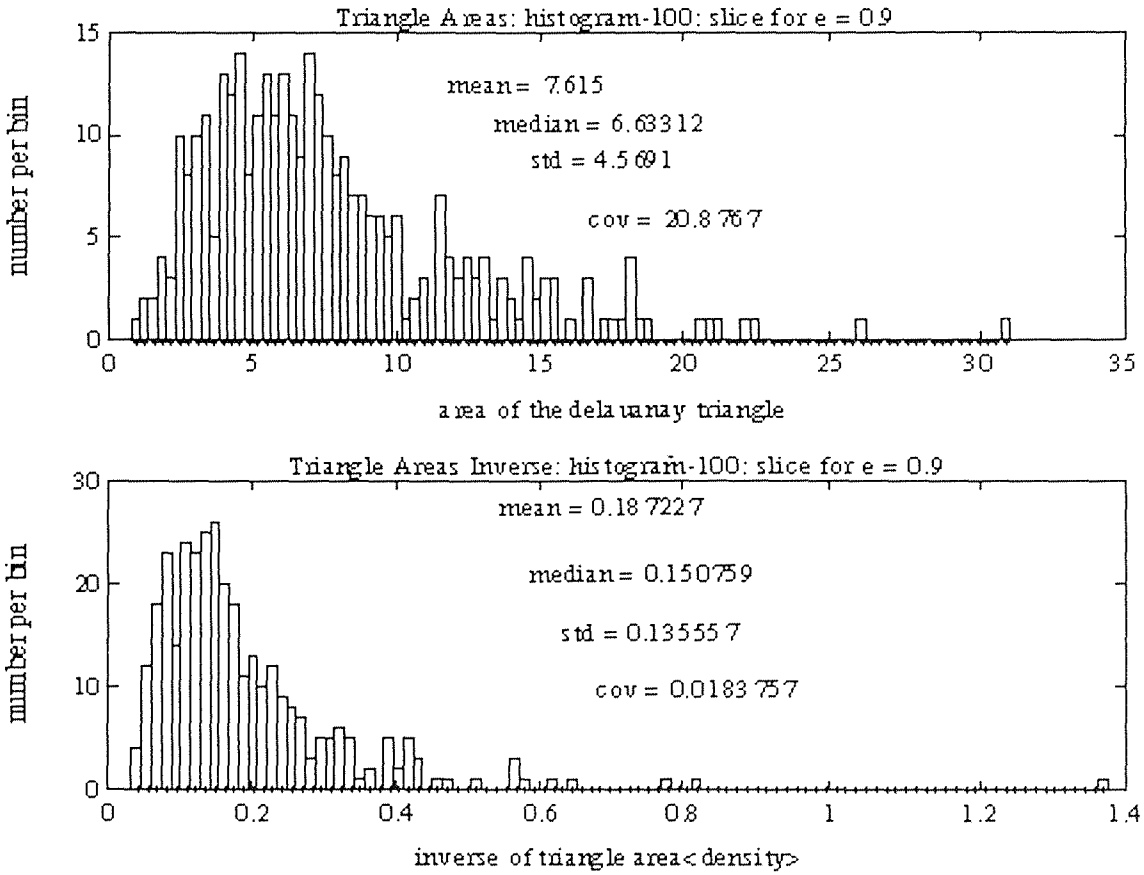

Figure D5 Histogram plot for Delaunay triangle areas and their inverses for e=0.9

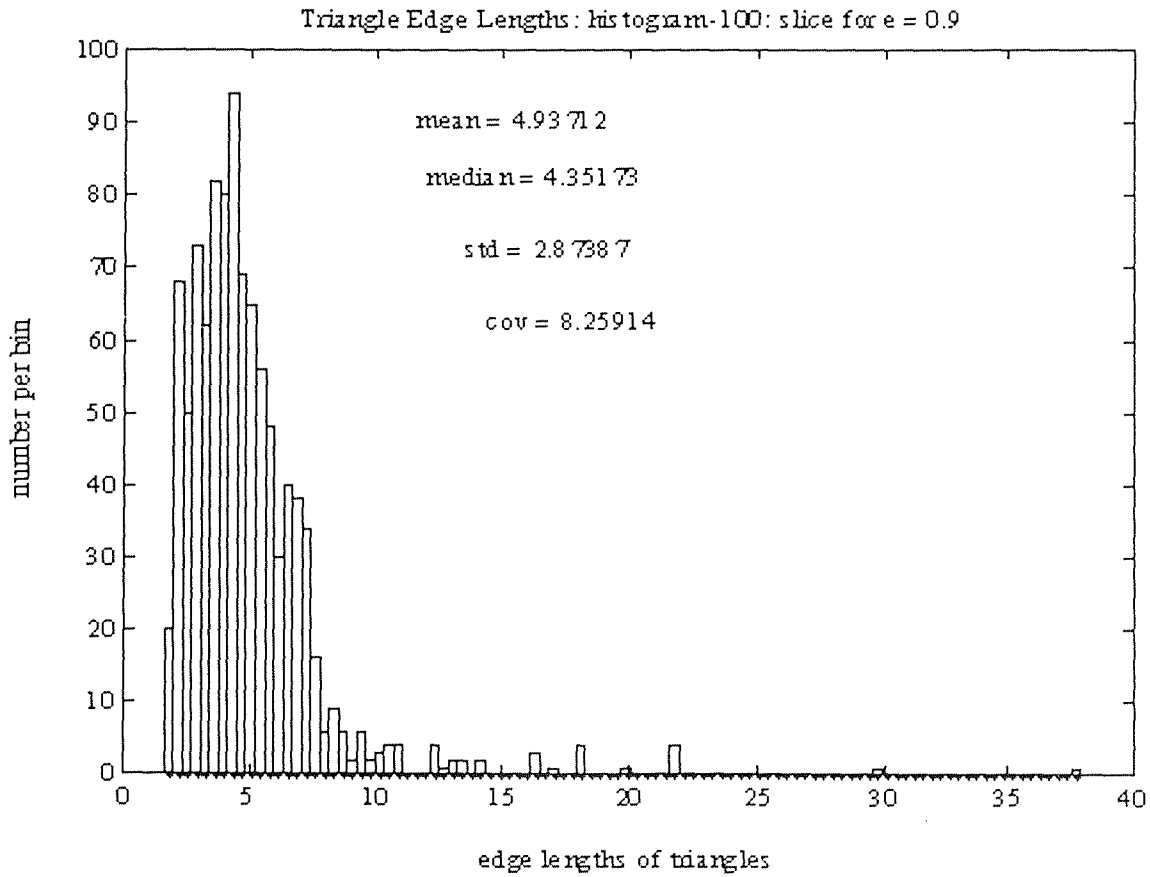

Figure D6 Histogram plot for Delaunay triangle edge lengths for e=0.9

REFERENCES

1. German, R. M. "Particle Packing Characteristics," *Metal Powder Industries Federation*, Princeton, NJ (1989).

2. Walton, O. R. "Numerical Simulation of Inelastic, Frictional Particle-Particle Interactions," in *Particulate Two-Phase Flow* (M. C. Roco edited) Chapter 25, Butterworth-Heinemann, Boston, (1992).

3. Campbell, C. S., "The effect of microstructure development on the collisional stress tensor in a granular flow, *Acta Mech.* 63, 61-72 (1986)

4. Hopkins, M. A. and Louge, M. Y., "Inelastic microstructure in rapid granular flows of smooth disks, *Phys. Fluids A* 3(1), 47-57(1991).

5. Kim, H. J, "Particle Dynamics Modeling of Boundary Effects in Granular Couette Flow", *PhD Dissertation* NJIT, Newark, NJ(1992).

6. Francis C. Moon, Chaotic Vibrations An Introduction for Applied Scientists and Engineers, John Wiley and Sons, New York (1987).

7. Hopkins, M. A., Jenkins, J. T. and Louge, M. Y., "On the structure of 3D shear flows", *Phys. Fluids A* 4(1), 37-49(1992).

8. Franco P. Preparata, and Michael Ian Shamos , Computational Geometry An Introduction, Springer Verlag, New York(1985).

9. Mandelbrot, B. B., Fractals, Form Chance and Dimension, W. H. Freeman, San Francisco, CA(1977).

10. Falconer, K., The geometry of fractal sets, Cambridge University Press, 1985.

11. Farmer, J. D., Ott, E., and Yorke, J. A., "The Dimension of Chaotic Attractors," *Physica* **7D**, 153-170, (1983).

12. Grassberger, P. and Proccacia, I., "Characterization of Strange Attractors," *Phys. Rev. Lett.* **50**, 346-349 (1983).

13. Liebovitch, L. S. and Toth, T., "A fast algorithm to determine fractal dimensions by box counting," *Phys. Lett. A* **141**(8,9) (1989).

14. Aurenhammer, F., "Voronoi Diagrams-A survey of a Fundamental Geometric Data Structure", *ACM Computing Surveys*, **23**(3) (1991).

15. Edelsbrunner, H., Algorithms in Combinatorial Geometry, Springer Verlag, New York(1987).

16 Ahuja, N., "Dot pattern processing using Voronoi polygons as neighborhoods", *IEEE Trans. Patt. Anal. Mach. Int. PAMI-4*, 336-343 (1982).

17. Sibson, R., "The Dirichlet tessellation as an aid in data analysis", *Scandinavian J. Statist.* vol. 7, pp. 14-20 (1980).

18. Henderson-Sellers, B., A book of object oriented knowledge, Prentice Hall, New York (1992).